Electronic Supplementary Information (ESI) for Lab on a Chip
This journal is © The Royal Society of Chemistry 2012

Electronic Supplementary Information

Dynamic trapping and high-throughput patterning of cells using pneumatic microstructures in a microfluidic device

Wenming Liu,[a] Li Li,[a] Jian-chun Wang,[a] Qin Tu,[a] Li Ren[a], Yaolei Wang[a] and Jinyi Wang*[ab]

[a] *College of Science and Veterinary Medicine, Northwest A&F University, Yangling, Shaanxi, 712100, China*

[b] *Shaanxi Key Laboratory of Molecular Biology for Agriculture, Yangling, Shaanxi, 712100, China*

Abstract. This supplementary information provides all the additional information and a more detailed discussion of the current study.

ESI Movies

Movie S1. Cell trapping of the U-PµS at the resting mode (0 psi pneumatic actuation and 10 µL/min flow). During the resting mode, no cells were captured in the U-PµS because of its two-dimensional structure.

Movie S2. Cell loss during the U-PµS trapping (4 psi pneumatic actuation and 40 µL/min flow). The trapped cells are easily removed in the initial-action mode of the U-PµS at a fast flow rate.

Movie S3. Cell trapping of the U-PµS at the initial-action mode (5 psi pneumatic actuation and 30 µL/min flow). The cells are smoothly captured in the U-PµS without leakage.

Movie S4. Hourglass-like cell loss during the U-PµS trapping with the initial-action mode at high-speed flow (5 psi pneumatic actuation and 200 µL/min flow). A higher flow rate can result in the leakage of the trapped cells, which is different from the cell loss observed at lower pneumatic actuation capture.

Movie S5. Path change of the flow in the full-action mode (15 psi pneumatic actuation and 120 µL/min flow). The U-PµS closes the road passage of the cell suspension, and that trapped cells are washed away at a high flow rate.

Movie S6. Cell trapping of the U-PµS in the full-action mode (10 psi pneumatic actuation and 120 µL/min flow). The back pressure at a high flow rate can allow flow passage to a certain extent through the U-PµS with lower pneumatic actuation in the full-action mode. The capture of several cells is also shown in this movie.

Movie S7. Mode conversion of the U-PµS for the withdrawal of the trapped cells. This movie presents a cleaning process of the trapped cells from the U-PµS by rinsing (120 µL/min) and a

mode conversion of the U-PµS from the initial-action mode to the resting mode (pneumatic

actuation from 5 to 0 psi). The U-PµS can realize a dynamic and precise positioning of cells.
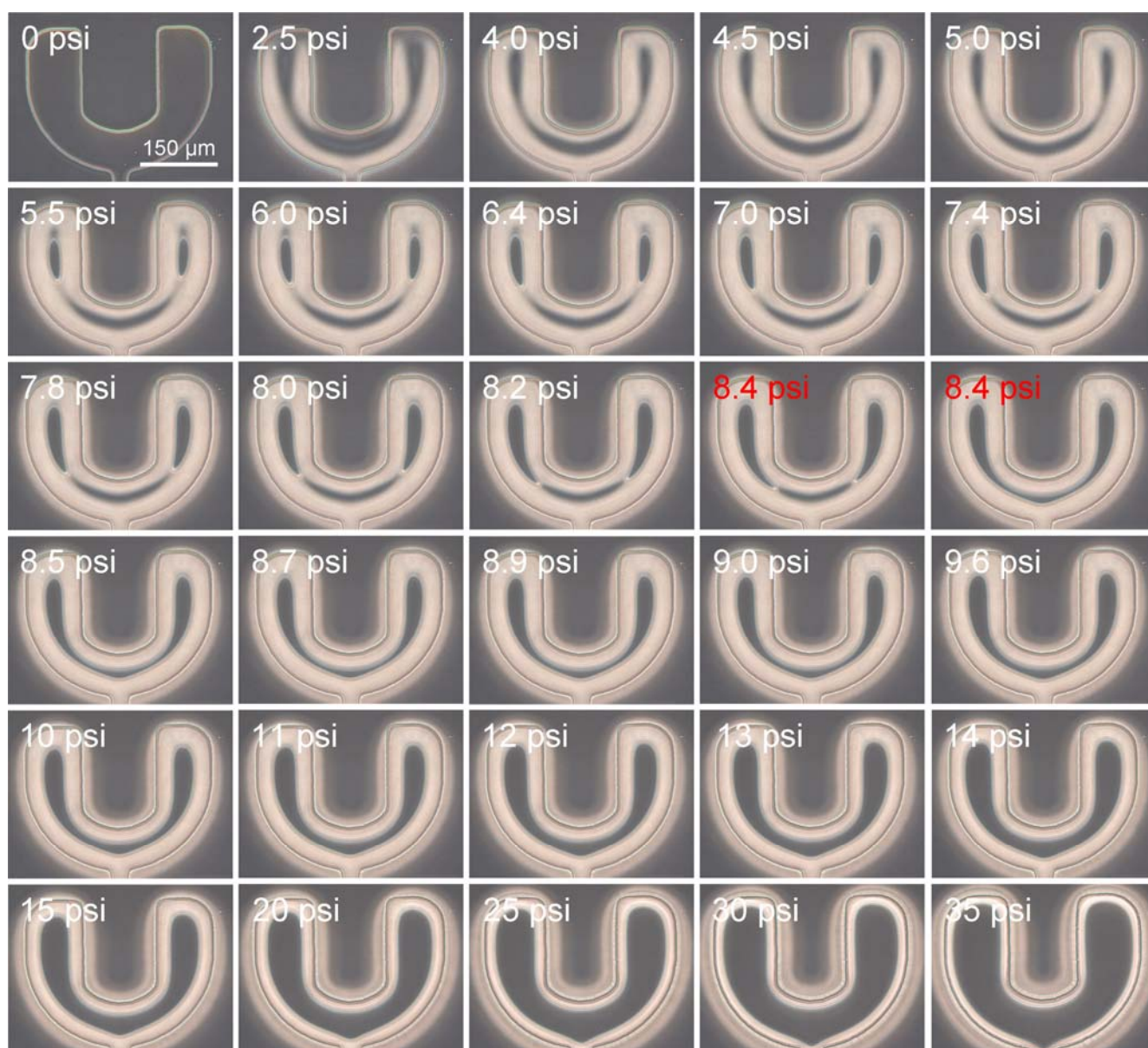
Fig. S1. Typical variable changes exhibited by the U-PµS under different air pressures (0 psi to 35 psi) and zero flow. First, a two-dimensional U-PµS was found at 0 psi pneumatic actuation. Second, a three-dimensional U-PµS appeared as the air pressure increased. The PDMS membrane was swollen with the sequential and observable displays from slight uplift with non-touching of the ceiling of the chamber (2.5, 4.0, 4.5, and 5.0 psi), to part uplift with both sides touching the ceiling of the chamber (5.5, 6.0, 6.4, 7.0, 7.4, 7.8, 8.0, 8.2, and 8.4 psi), as well as to entirely uplift with U-shaped array touching the ceiling of the chamber (8.4, 8.5, 8.7, 8.9, 9.0, 9.6, 10, 11, 12, 13, 14, 15, 20, 25, 30, and 35 psi). Red-labelled images

present the qualitative U-PµS shape alteration from both sides touching the ceiling of the

chamber to the U-shaped array touching at 8.4 psi pneumatic actuation. These pictures

demonstrate that a higher pneumatic actuation can lead to a higher-grade membrane

deformation, and the nonuniform design of the U-PµS results in its various shape exhibitions

along with the different pneumatic actuations. The results above were determined based on

the refractive appearance of the U-PµS as shown in the optical microscope system (Olympus,

CKX41). The method was repeated thrice using six batches of the fabricated devices. The

pneumatic range of different U-PµS states was described as mean ± S.D. psi in the current

paper.
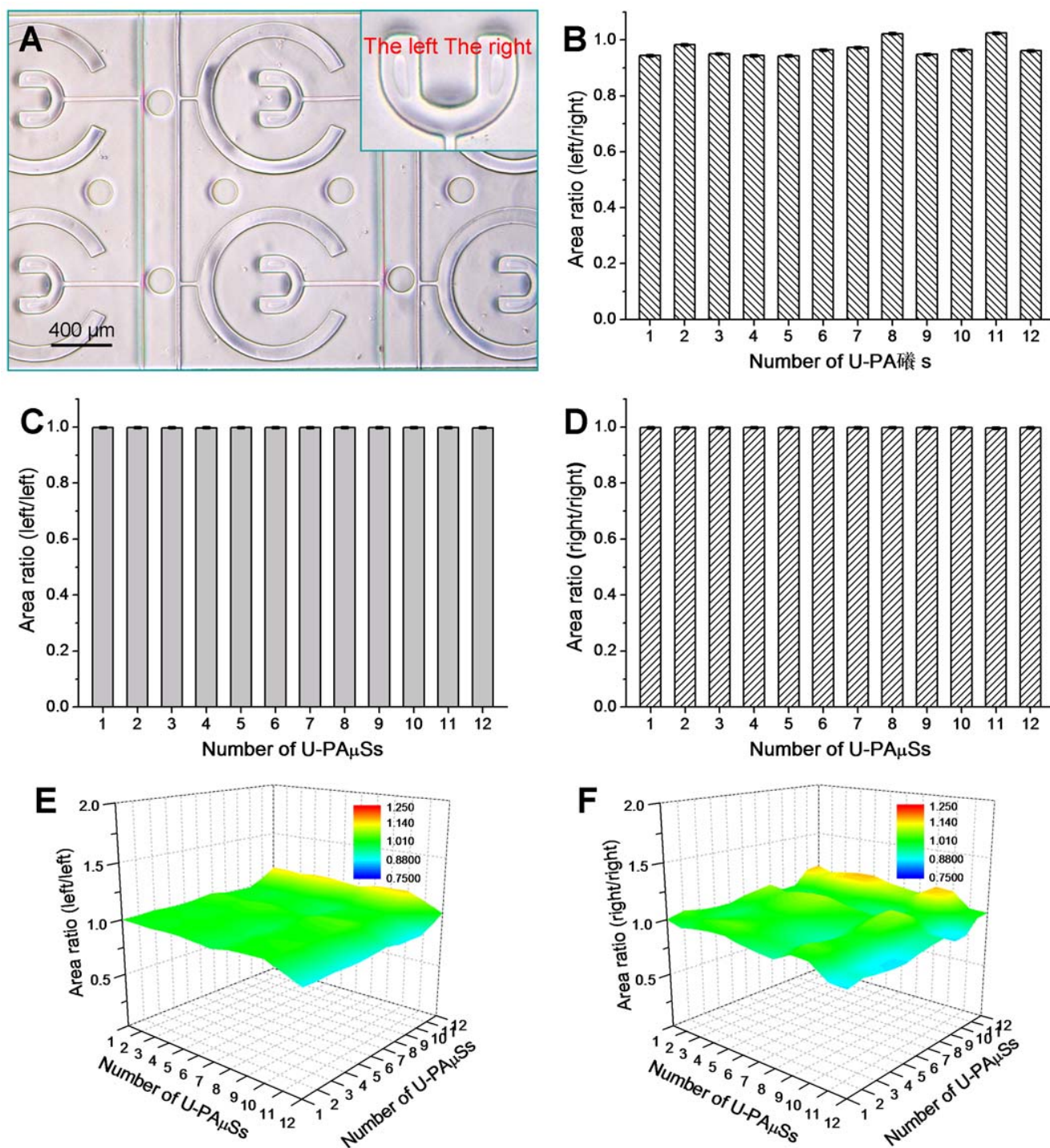
Fig. S2. Spatial consistency assessment of the U-PµSs in the microfluidic device. (A) Optical image of the actual U-PµSs (7.3 psi pneumatic actuation and 0 µL/min flow). Inset shows the enlarged picture of the U-PµS. (B) Area ratios of the left and right sides. The areas point to the touching areas of the U-PµSs to the ceiling of the microchamber. In this pneumatic actuation, both sides of the microstructures were in contact with the ceiling (defined here as the left and

the right, which correspond to the inset of A). Their touching areas were determined to

investigate the three-dimensional structure consistency of the U-PµSs because it is

convenient for quantitative calculation. (C) Area ratios of each of the two lefts of the U-PµS

between two pneumatic actuations. (D) Area ratios of each of the two rights of the U-PµS

between two pneumatic actuations. (E) Area ratios of the lefts between each of the two

U-PµSs. (F) Area ratios of the rights between each of the two U-PµSs. The results show that

the spatial structure of the U-PµSs is consistent and well controlled. This condition suggests

that the U-PµSs are potentially fit to complete high-throughput cell trapping in a quantitative

uniform manner. Twelve U-PµSs were applied for the current tests including the six U-PµSs

showed in this figure A. All the data were from at least three repeated tests.
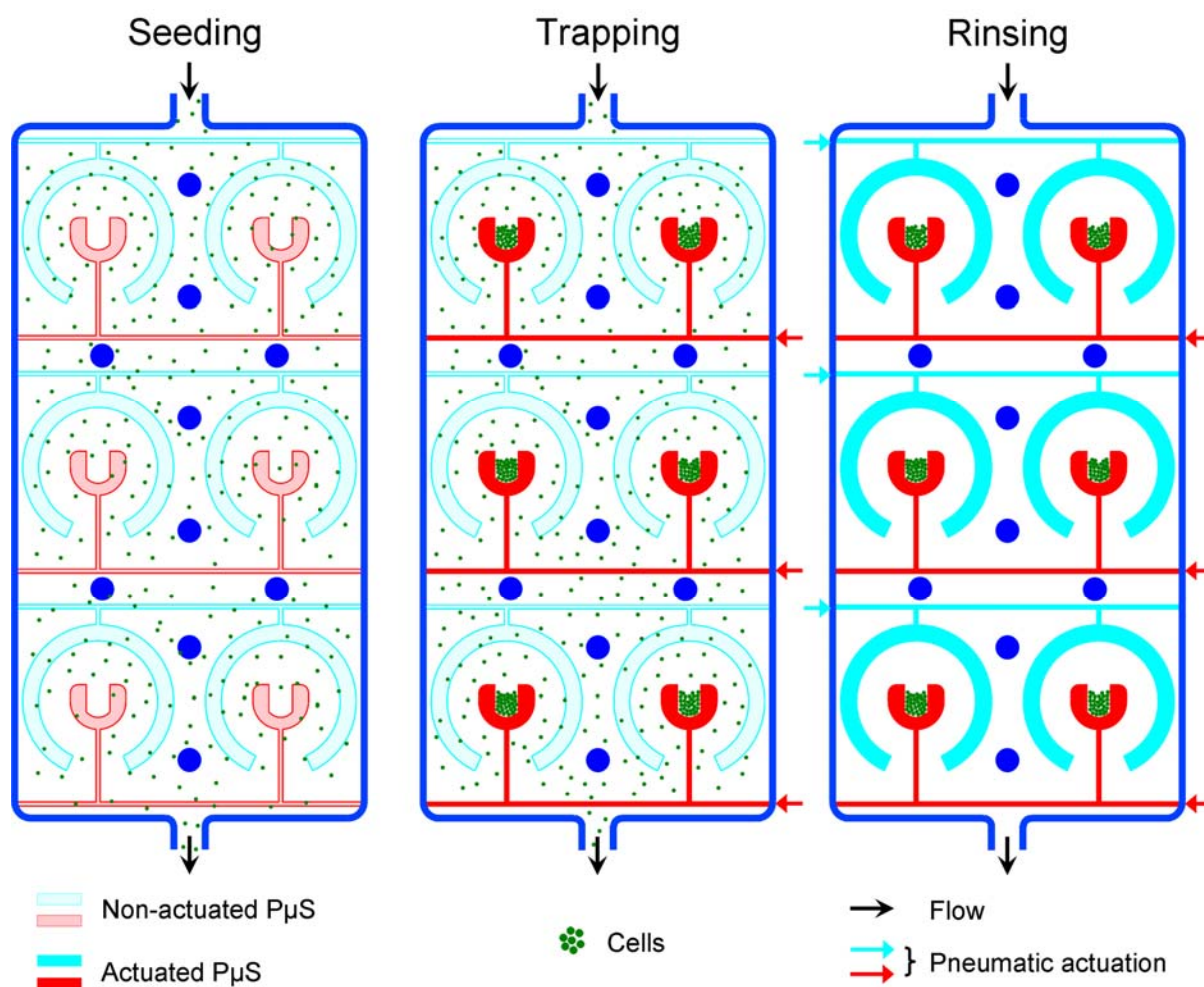
Fig. S3. Schematic diagrams of the cell trapping process using U-PµSs. During trapping, U-PµSs were actuated (red) from the resting state (light red). In addition, the umbrella-like PµSs were actuated (cyan) for a special protection of the trapped cells during the rinsing step.
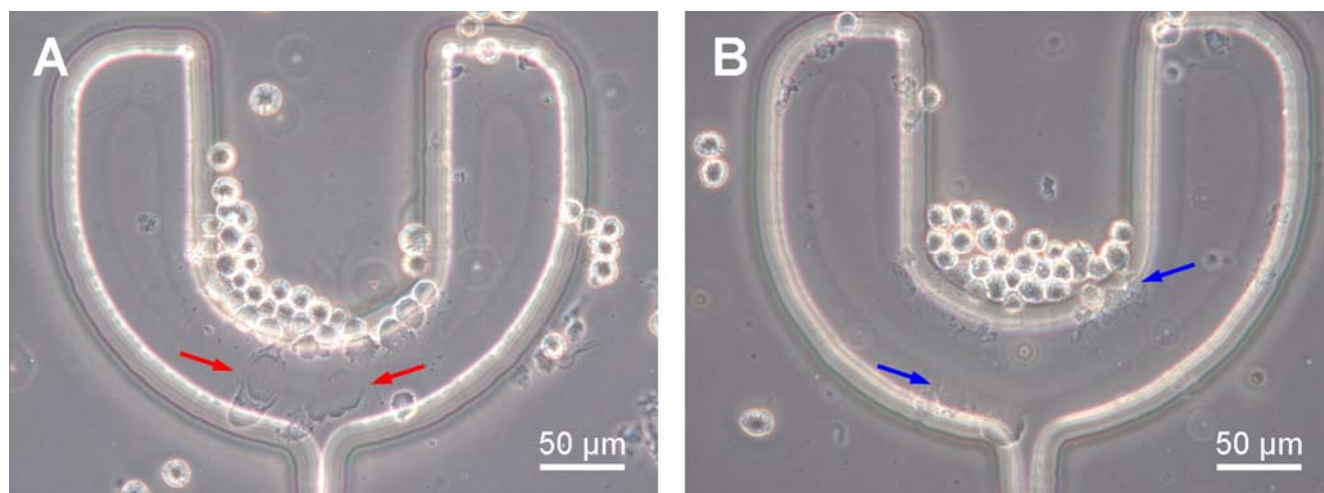
Fig. S4. Cell deformation during U-PµS trapping at a high flow rate and high pneumatic actuation. (A) Cell trapping at 12 psi pneumatic actuation and 250 µL/min flow. Several cells were obviously deformed (red arrows) in the gap between the U-PµS and the ceiling of the microchamber. (B) Cell trapping at 15 psi pneumatic actuation and 400 µL/min flow. Blue arrows show the cell debris. These results suggest that high flow rates and high pneumatic actuations could potentially result in the serious injury and direct necrosis of several cells. These conditions are not suitable for further applications involving live cell research, especially on the studies of cell function and behavior.
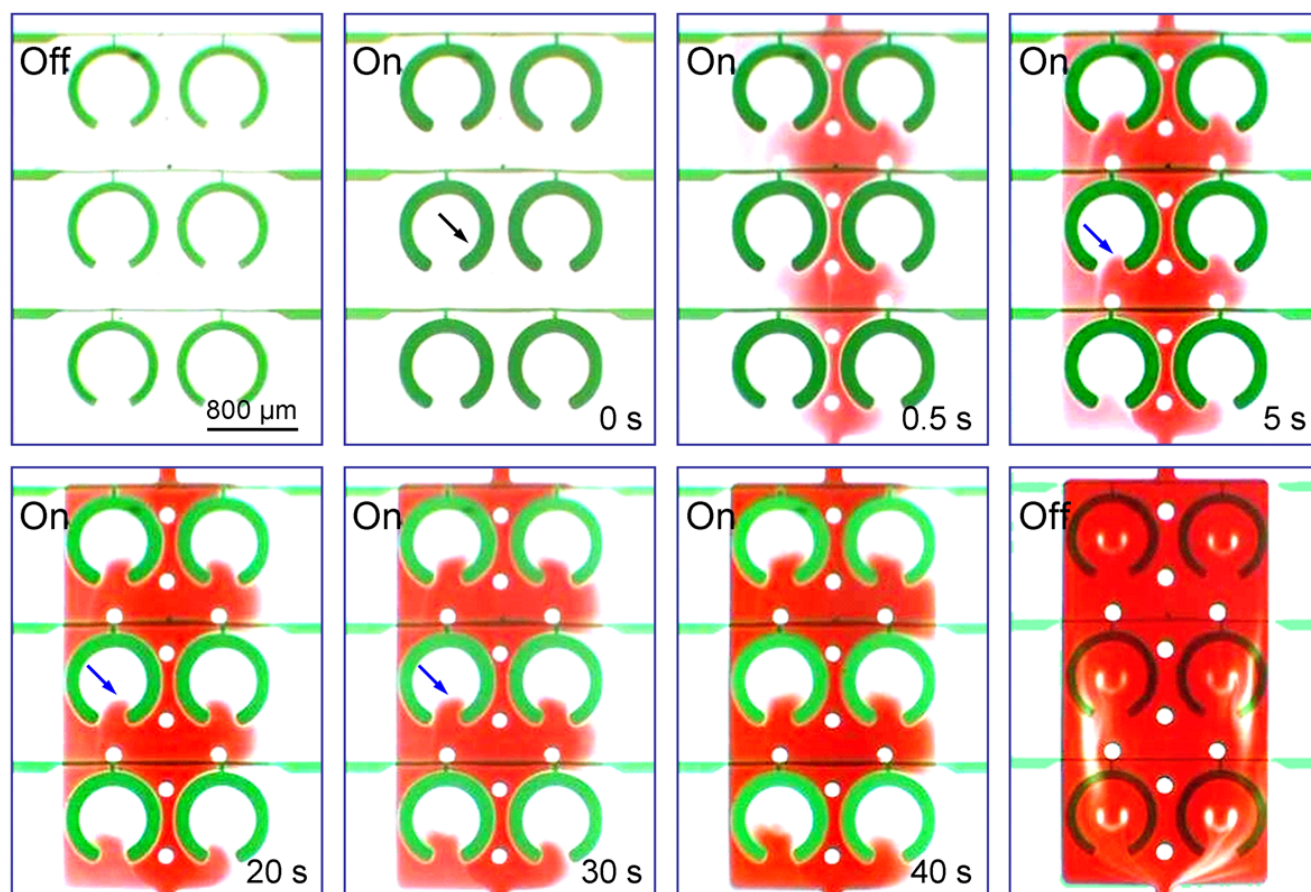
Fig. S5. Hydrodynamic blocking of the flow using the on/off switch of the umbrella-like PµSs. During pneumatic actuation (on, 30 psi), the umbrella-like PµSs expanded (black arrow) and served as physical barriers, and resulted in a detour of flow (red, 120 µL/min). That is, the fluid cannot positively enter into the U-PµSs. Time lapse images show that the communication between the environments of the inner U-PµSs and flow mainly depends on molecular diffusion (blue arrows), implying that a nearly zero flow condition exists around the U-PµSs. Therefore, the actuated umbrella-like PµSs can prevent the negative effects of the flow on the trapped cells. In addition, during the cancellation of actuation (off, 0 psi) of the umbrella-like PµSs, the static flow condition around U-PµSs is replaced immediately by the perfusion flow. These results demonstrate that the on-demand protection of the trapped cells could be simply and conveniently realized via a real-time actuation of the umbrella-like PµSs.
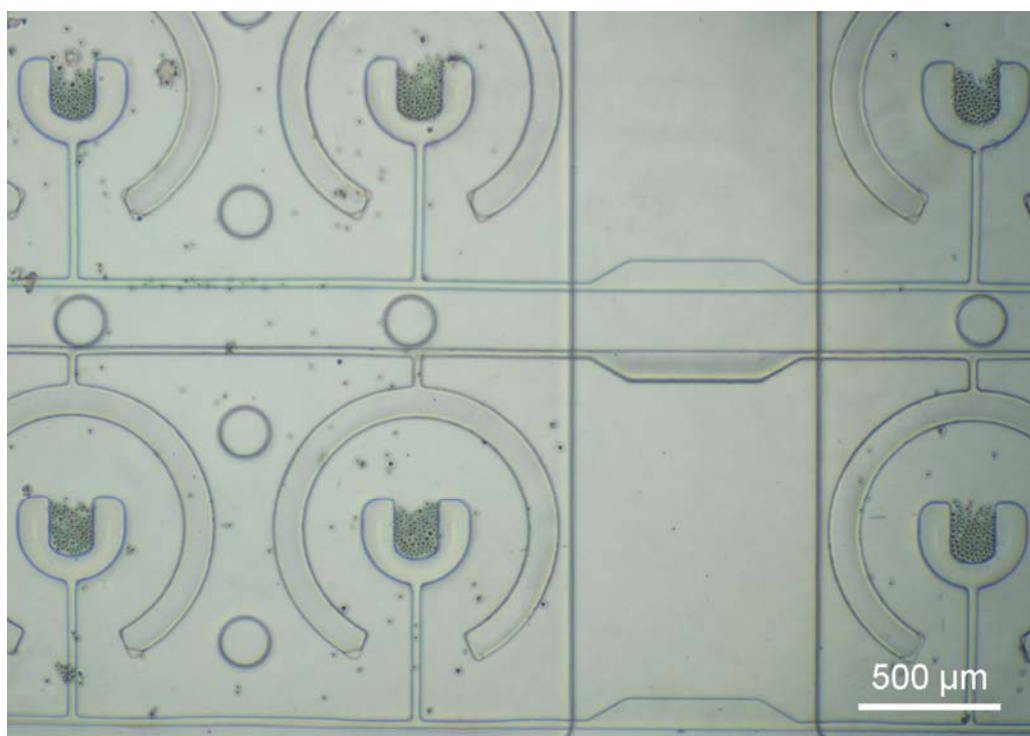
Fig. S6. Parallel trapping of human hepatocellular liver carcinoma HepG2 cells using the

U-PµS arrays at 6 psi pneumatic actuation and 30 µL/min flow.

11